Pergamon

Journal of Structural Geology, Vol. 20, No. 9/10, pp. 1229 to 1245, 1998

0191-8141/98/$ - see front matter

PII: S0191-8141(98)00060-1

Sigmoidal structures featuring dextral shear during emplacement of the Hercynian granite complex of Cauterets–Panticosa (Pyrenees)

GERARD GLEIZES* and DENIS LEBLANC

Laboratoire de Pétrophysique et Tectonique, UMR 5563 CNRS, Université Paul-Sabatier, 38 rue des Trente-Six-Ponts, 31400, Toulouse, France

VICENTE SANTANA

Departamento de Estratigrafia, Geodinomica y Paleontologia, Universidad del Pais Vasco, Ap. 644, Bilbao, 48080, Spain

and

PHILIPPE OLIVIER* and JEAN LUC BOUCHEZ*

Laboratoire de Pétrophysique et Tectonique, UMR 5563 CNRS, Université Paul-Sabatier, 38 rue des Trente-Six-Ponts, 31400, Toulouse, France

(*Received* 1 *July* 1997; *accepted in revised form* 20 *April* 1998)

Abstract—The three plutons of the Cauterets–Panticosa granite complex are studied by the anisotropy of magnetic susceptibility (AMS) technique. As expected from the dominantly paramagnetic nature of the rocks, the magnetic susceptibility zonation accurately compares with the lithological zonation. Detailed examination of the linear and planar structural patterns of the plutons allows the difficult problem of their formation mechanisms to be explored. The sigmoidal pattern of the linear structures only results from regional tectonics and points unequivocally to a dextral shear component for the responsible tectonic event. The concentric planar structures, while also affected by regional tectonics, retain some imprint of magma emplacement. The microstructures observed in the granitoids point to a continuous deformation from the magmatic state to the high-temperature solid state. In the country rocks, structures and kinematic criteria underline the transpressive character of the D_2 Hercynian event of the Pyrenees which resulted in a partitioning between zones where either compression or dextral strike-slip were dominant. All these data constrain a new model of D_2 syn-tectonic emplacement for the plutons of the Cauterets–Panticosa complex and remarkably illustrate structural features resulting from a transpressive regime.

INTRODUCTION

The petrography of the Cauterets–Panticosa granitic complex is one of the best known of the Pyrenees granites (Debon, 1972, 1980). The complex was first considered to be syn-tectonic on the basis of field structural observations in the country rocks (Mirouse, 1966; Valéro, 1974; Moreau, 1975). In contrast, Debon (1975) proposed that the complex was emplaced after the so-called D_2 main phase of the regional Hercynian orogeny, by means of forceful intrusions and subsequent collapse of their roof. However, the lack of data on the internal structures of the complex meant that this model was hypothetical.

In order to determine the internal structures, we applied the anisotropy of magnetic susceptibility (AMS) methods (Bouchez, 1997), which have now routinely been used on granitic plutons for the past 10 years, to the Cauterets–Panticosa complex. The AMS efficiency in determining the internal structures of plutonic rocks, especially the lineations which are difficult to determine in the field, has been demonstrated in plutons of different ages and levels of emplacement in the crust throughout the world (e.g. in Brazil by Archanjo *et al.*, 1994; in Canada by Cruden and Launeau, 1994; in Nigeria by Ferré *et al.*, 1995; in California by Saint-Blanquat and Tikoff, 1997; among the most recent studies). These studies revealed that the granitoid plutons display well-organized structures which record the deformation related to late stages of upwelling and/or to tectonic movements coeval with magma emplacement.

In the Pyrenees, such studies, performed in some of the numerous Hercynian plutons, have demonstrated that their emplacement was syn-tectonic (Leblanc *et al.*, 1994; Gleizes *et al.*, 1997). In addition, by specifying, in both plutons and country rocks, the geometry

*E-mail: gleizes/olivier/bouchez@lucid.ups-tlse.fr

and kinematics of the structures associated with pluton emplacement, recent studies (Leblanc *et al.*, 1996; Evans *et al.*, 1997) have precisely related the magmatic and post-magmatic structures of the plutons to the regional tectonic events.

Our new structural data collected in the Cauterets–Panticosa complex and its country rocks provide evidence of emplacement of the magma coeval with a dextral compressive deformation event, called D_2, that affected the whole chain. This constrains a model of regional dextral transpressive regime for the setting of the complex.

GEOLOGICAL SETTING

The Cauterets–Panticosa calc-alkaline and aluminous granitic complex occupies an area of more than 250 km^2 in the western Axial Zone of the Pyrenees. The complex results from the juxtaposition of three plutons (Fig. 1). The Panticosa pluton crops out essentially in Spain, and the two Cauterets plutons, to the west and east, which will be referred to as W-Cauterets and E-Cauterets, partly belong to the famous 'Parc National des Pyrénées' in France. The plutons display a concentric compositional zoning (Debon, 1972) and are intrusive into folded pelite, limestone and quartzite formations, mostly of Devonian age. Carboniferous flysch is also present, but at some distance from the northern border of the Cauterets plutons. All these sediments are metamorphosed within the chlorite zone of the greenschist facies. A contact metamorphic aureole, superimposed on the regional metamorphism, extends around the whole complex (Fig. 1).

The regional foliations of the country rocks, attributed to the main Hercynian phase D_2 (Zwart, 1979), have average strikes of around N110°E and steep northward to subvertical dips (Debon, 1972). Trajectories of foliation traces wrap the plutons and locally form triangular neutral zones (Fig. 1). The fold axes, reported after Wensink (1962) and Mirouse (1966), trend parallel to the main foliation trace and also to the borders of the plutons in map view. These D_2 Hercynian structures are disturbed by Alpine S-verging thrust faults, the best known of which is the Gavarnie thrust (Bresson, 1903) for which the minimum horizontal displacement reaches 6 km in map view. Although the Hercynian zones of localized strain are usually wider and deform the rocks more penetratively than the Alpine fault zones, distinction between them may be difficult as some of the Hercynian shear zones have been re-used by the Alpine faults with the same apparent kinematics.

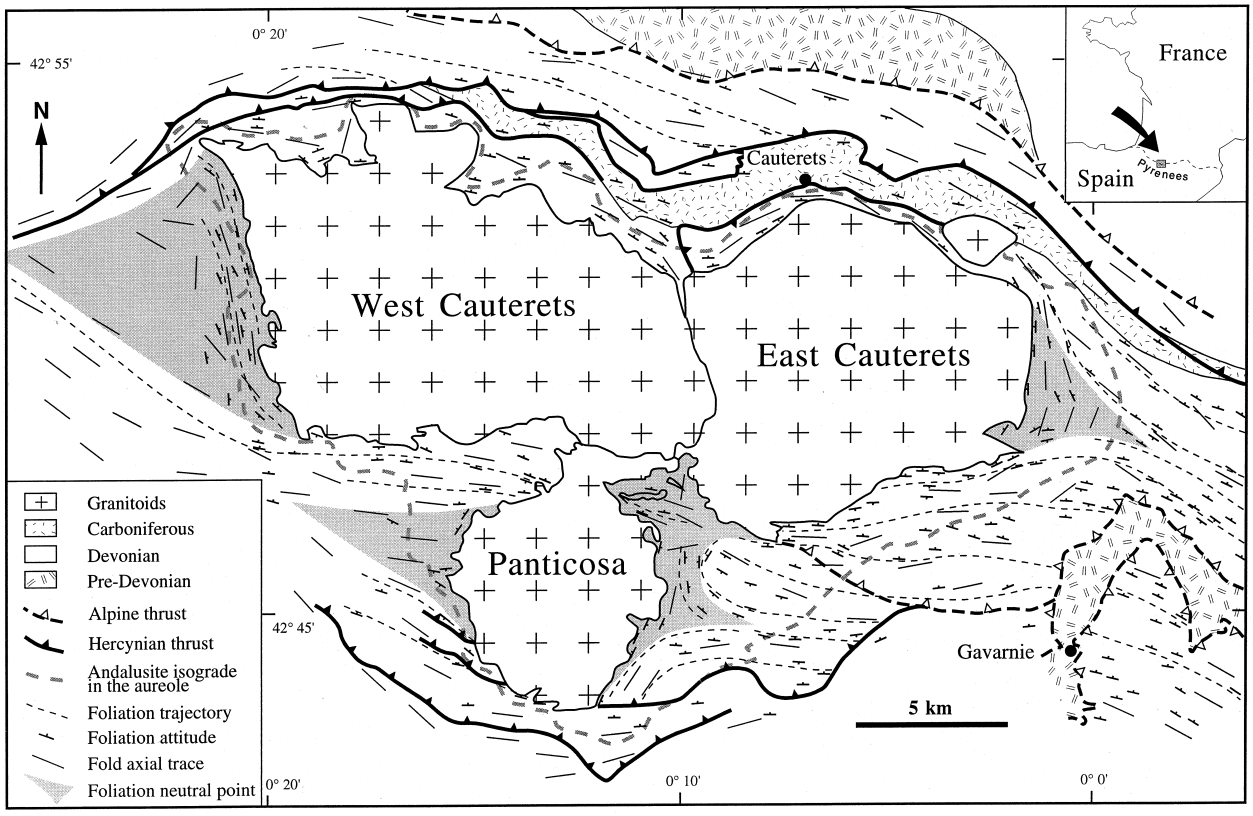

Fig. 1. Geological map of the Cauterets–Panticosa area, interpreted by using data from the 1/50,000 geological maps of Vielle-Aure and Argelès-Gazost (French Geological Survey), and also from Wensink (1962), Mirouse (1966) and Debon (1972).

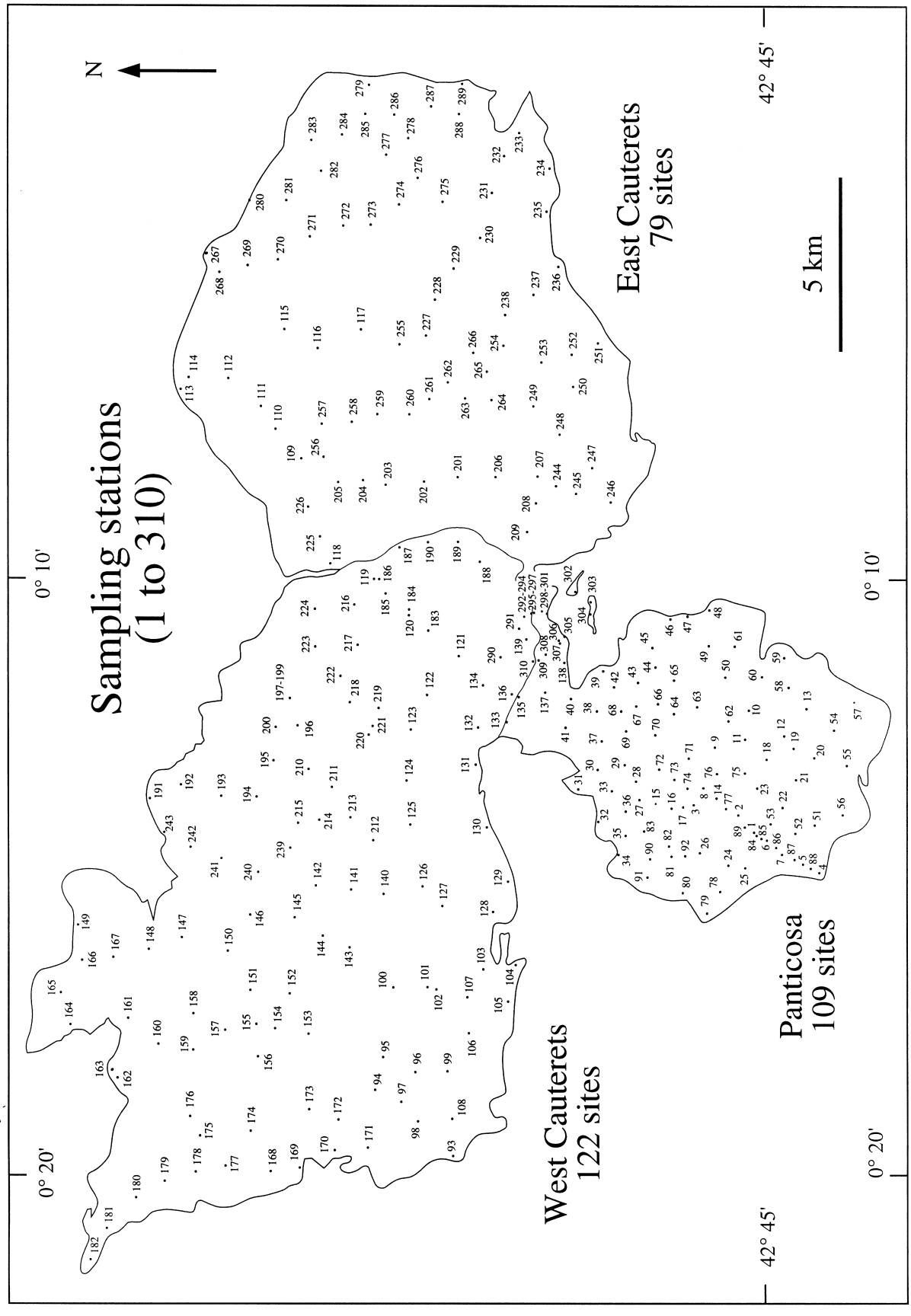

Fig. 2. Location of the sampling stations in the Cauterets–Panticosa complex.

Table 1. AMS data for the 310 sampling stations*

Site	K (10^{-5} SI)	K_1	K_3	P_{para}%	Site	K (10^{-5} SI)	K_1	K_3	P_{para}%	Site	K (10^{-5} SI)	K_1	K_3	P_{para}%	Site	K (10^{-5} SI)	K_1	K_3	P_{para}%	Site	K (10^{-5} SI)	K_1	K_3	P_{para}%
1	18.6	276/15	172/40	2.2	63	23.7	144/55	316/38	1.9	125	8.5	219/31	78/59	1.7	187	9.2	85/48	261/41	3.0	249	48.5	258/43	158/1	2.9
2	11.6	283/36	145/46	2.8	64	23.7	226/19	93/63	4.0	126	8.3	262/41	59/49	2.7	188	7.2	*	310/33	2.1	250	45.4	278/32	185/3	7.8
3	8.7	243/70	155/0	2.0	65	22.6	239/30	337/15	3.5	127	20.2	277/19	*	4.0	189	7.7	40/7	305/34	3.4	251	23.7	247/15	345/27	10.6
4	34.1	30/64	222/23	1.8	66	24.6	233/28	332/16	4.6	128	21.4	249/19	161/4	2.6	190	7.7	50/32	300/32	2.9	252	54.7	244/25	342/11	3.6
5	55.2	119/4	215/28	9.1	67	30.3	242/49	356/18	4.8	129	8.4	248/39	12/36	2.4	191	6.8	264/7	160/38	3.0	253	31.0	60/24	161/33	4.5
6	22.8	277/6	194/47	3.3	68	36.1	279/14	191/10	1.7	130	39.1	258/30	10/32	2.2	192	18.2	88/4	182/38	2.7	254	23.2	268/12	173/21	2.2
7	34.8	31/11	143/69	3.4	69	29.9	201/68	342/18	3.7	131	17.7	222/45	129/2	5.3	193	7.6	351/42	154/43	1.2	255	4.6	39/56	201/33	2.0
8	6.3	202/32	95/24	5.3	70	16.6	123/5	230/80	3.5	132	11.2	96/62	229/8	2.3	194	7.7	247/4	153/38	2.1	256	25.3	204/20	313/46	1.8
9	14.0	222/38	346/34	2.1	71	12.6	113/34	332/58	2.6	133	44.2	82/42	233/43	2.9	195	7.7	80/1	177/63	2.9	257	19.3	212/60	111/6	2.0
10	20.5	197/53	86/17	2.0	72	13.9	245/23	132/42	2.8	134	9.2	221/46	4/36	3.5	196	8.8	62/38	221/53	2.7	258	20.2	354/63	258/4	2.1
11	16.2	82/20	313/60	2.5	73	7.9	200/4	354/86	2.9	135	37.5	63/32	193/45	4.3	197	7.9	289/49	174/20	5.2	259	21.1	15/4	281/50	3.0
12	16.2	231/51	322/37	1.5	74	13.2	133/60	307/31	2.0	136	8.3	†	339/19	1.5	198	0.8	72/64	185/11	8.7	260	22.6	245/35	28/48	3.2
13	24.1	347/83	122/3	2.0	75	16.1	234/21	324/13	1.9	137	38.8	285/36	90/56	1.8	199	5.6	18/30	192/62	2.5	261	17.3	231/9	120/66	3.1
14	8.2	255/6	351/51	4.7	76	7.2	230/21	337/37	2.8	138	39.1	314/80	45/0	5.6	200	17.5	84/34	219/46	4.3	262	22.9	†	†	2.1
15	7.3	221/36	1/54	3.1	77	11.0	242/16	136/41	3.4	139	9.0	241/37	349/23	3.8	201	26.4	48/6	312/46	2.9	263	41.6	231/23	85/64	3.2
16	7.4	110/26	1/28	3.9	78	26.3	62/77	244/12	1.7	140	4.5	275/19	60/68	4.5	202	24.3	25/8	290/39	3.1	264	27.9	239/32	98 /52	2.6
17	7.7	233/13	356/69	5.5	79	27.1	308/1	39/44	2.7	141	6.9	263/36	54/53	3.0	203	25.4	205/10	303/37	3.0	265	23.1	264/12	359/16	2.7
18	15.3	242/11	151/45	3.0	80	24.1	135/22	225/9	1.3	142	7.4	250/57	†	2.0	204	25.6	32/14	277/57	2.4	266	25.2	33/21	181/64	2.2
19	19.3	234/32	121/31	3.0	81	18.2	93/41	297/62	2.1	143	6.9	222/31	77/54	3.0	205	27.4	26/19	271/53	1.7	267	36.6	150/42	353/29	1.3
20	24.3	254/3	150/71	4.4	82	9.4	264/6	354/36	1.4	144	9.1	244/63	71/27	3.9	206	36.3	206/22	305/20	3.1	268	28.7	275/27	18/25	2.3
21	16.6	9/22	196/76	3.5	83	8.2	213/21	328/44	2.3	145	10.7	303/27	65/49	4.0	207	53.8	†	91/31	3.2	269	26.3	311/40	197/27	1.8
22	13.8	259/19	154/39	2.7	84	21.0	269/30	152/39	3.5	146	7.9	23/4	116/40	2.8	208	25.8	307/22	207/35	4.5	270	21.5	46/24	263/56	1.0
23	11.2	236/24	145/13	3.1	85	23.7	263 /14	153/50	3.7	147	6.7	†	155/37	2.7	209	23.6	221/29	315/6	1.7	271	24.6	93/10	182/0	1.0
24	16.6	29/36	161/43	5.9	86	25.3	306/22	180/51	3.0	148	19.0	41/22	316/1	3.1	210	5.0	89/24	281/65	4.3	272	20.1	49/43	223/45	3.1
25	23.3	103/2	294/86	2.3	87	46.1	341/32	110/47	8.2	149	26.2	59/16	150/26	2.4	211	9.2	89/0	179/62	2.2	273	21.0	257/28	86/59	3.7
26	13.1	91/3	357/21	4.3	88	60.9	129/4	247/76	7.2	150	12.7	†	130/27	5.4	212	8.4	211/21	52/68	3.5	274	19.6	46/47	284/25	1.6
27	16.8	226/10	321/33	3.3	89	18.2	273/22	174/22	3.5	151	8.3	287/67	87/20	2.1	213	5.6	297/3	193/80	2.5	275	24.2	228/16	128/21	1.5
28	11.6	220/15	123/24	3.1	90	23.0	198/14	103/2	2.3	152	7.7	258/38	112/48	2.5	214	11.3	231/42	†	2.1	276	24.7	231/6	136/41	2.6
29	19.6	222/28	326/28	5.2	91	24.2	192/63	298/9	2.4	153	19.2	247/26	23/56	3.1	215	3.9	90/11	292/72	4.4	277	27.9	183/0	96/29	2.0
30	28.1	206/22	327/51	4.8	92	14.4	2/3	98/22	0.8	154	17.1	221/60	40/32	2.6	216	8.0	46/58	253 /29	3.2	278	30.3	178/20	87/2	3.3
31	34.9	201/30	302/19	3.5	93	13.3	290/64	45/11	3.4	155	18.2	295/49	92/39	2.6	217	8.2	87/15	263/75	4.6	279	35.0	173/16	76/23	1.9
32	29.1	214/12	310/22	2.6	94	8.8	192/33	78/30	2.5	156	18.3	307/55	104/34	3.3.	218	6.7	279/6	148/82	3.6	280	32.4	127/15	28/30	3.7
33	20.1	222/8	317/36	3.9	95	14.6	293/27	30/14	2.7	157	18.0	284/66	95/23	2.3	219	8.3	253/7	96/83	2.7	281	23.2	302/13	31/7	2.6
34	37.6	39/40	155/30	2.1	96	18.7	306/46	177/31	5.7	158	18.9	16/36	166/50	2.8	220	10.7	288/25	†	2.6	282	29.9	56/74	205/22	2.3
35	23.5	214/2	305/4	3.3	97	23.6	305/36	45/4	6.3	159	18.6	359/36	101/16	3.7	221	9.8	297/6	69/78	3.5	283	34.5	152/72	37/11	2.6
36	27.1	204/12	296/16	3.6	98	35.3	115/49	219/12	4.3	160	17.9	4/40	149/45	3.3	222	10.0	68/20	206/65	3.2	284	30.0	310/50	70/21	2.0
37	23.0	233/16	339/49	3.0	99	18.8	279/21	29/23	4.6	161	11.6	39/45	160/27	6.8	223	17.7	42/34	240/55	3.6	285	35.2	283/18	†	1.9
38	34.2	240/13	335/21	6.8	100	18.9	268/41	21/19	3.8	162	10.2	22/49	161/33	7.7	224	18.6	27/54	253/29	2.2	286	33.1	222/21	116/26	2.2
39	36.5	218/30	125/19	2.6	101	17.7	279/27	16/13	4.6	163	10.0	52/12	157/50	3.1	225	31.5	39/42	288/20	1.2	287	34.6	29/24	130/17	1.3

40	35.3	107/54	359/15	3.7	102	8.8	285/21	21/17	10.0	164	48.0	343/19	251/6	0.6	226	28.8	118/52	292/39	1.8	288	32.5	41/56	151/12	2.2
41	39.7	338/86	183/4	6.9	103	12.7	240/45	1/27	11.7	165	25.9	45/24	142/13	1.6	227	9.0	58/10	157/41	2.7	289	26.3	43/33	289/34	1.3
42	36.4	249/41	357/16	6.1	104	8.5	261/17	359/28	2.0	166	26.5	52/26	314/15	1.4	228	48.7	210/18	18/72	4.9	290	12.7	248/25	111/58	4.0
43	32.7	247/43	359/23	4.8	105	9.7	266/28	2/23	7.8	167	9.6	59/6	154/36	3.1	229	32.5	24/60	185/29	6.1	291	8.4	252/16	5/52	2.0
44	26.9	249/53	358/13	6.2	106	14.7	210/54	24/35	10.8	168	7.5	335/36	68/6	3.2	230	22.6	63/9	156/5	2.0	292	9.4	58/2	146/29	2.7
45	29.4	128/43	342/42	2.0	107	13.5	†	49/48	8.1	169	11.7	342/2	72/9	2.4	231	31.0	58/0	146/44	3.7	293	10.8	244/11	356/51	3.1
46	35.5	139/49	334/39	3.9	108	24.1	325/44	209/24	4.9	170	8.3	323/26	231/1	2.1	232	34.2	60/48	174/17	2.7	294	6.5	256/8	5/64	2.6
47	31.1	125/46	317/44	8.4	109	22.7	41/24	133/1	1.9	171	10.6	340/36	236/23	2.0	233	31.1	243/26	138/28	2.9	295	42.6	89/10	189/39	2.4
48	37.6	200/52	83/19	4.5	110	23.7	247/22	154/13	1.7	172	8.1	265/63	49/21	3.1	234	28.6	232/21	120/43	2.6	296	10.3	256/15	157/54	3.8
49	24.6	129/50	280/36	4.5	111	23.4	66/8	158/14	1.7	173	9.4	340/58	233/9	2.4	235	32.2	247/23	143/30	1.9	297	8.9	55/13	322/5	3.0
50	22.2	62/14	319/47	1.9	112	24.7	257/25	350/9	1.9	174	27.3	†	264/2	1.8	236	24.1	62/28	154/3	5.5	298	42.8	†	†	2.0
51	27.8	23/71	176/17	3.5	113	26.7	281/42	172/20	1.4	175	8.4	352/1	86/84	3.5	237	31.2	231/22	137/10	3.2	299	41.2	289/21	147/64	3.6
52	22.6	54/59	169/16	2.7	114	24.5	39/59	170/24	1.9	176	11.1	7/10	267/42	3.5	238	24.9	229/17	139/3	2.9	300	39.1	13/41	261/29	2.2
53	24.9	289/15	177/64	3.4	115	21.9	89/33	180/3	2.0	177	8.3	218/67	74/20	5.6	239	2.8	290/22	96/68	3.7	301	43.5	47/36	152/26	2.9
54	27.0	351/68	108/12	2.2	116	18.5	306/78	174/10	3.4	178	8.7	307/62	70/16	5.5	240	8.4	19/9	113/12	2.1	302	35.8	233/26	326/5	2.5
55	29.8	274/24	151/51	3.4	117	18.5	245/12	136/53	2.9	179	9.5	355/44	250/11	2.6	241	17.6	27/25	155/54	3.1	303	32.4	210/32	318/27	9.0
56	31.5	280/39	165/28	2.7	118	31.1	35/1	305/48	1.5	180	8.4	325/82	81/4	3.6	242	19.6	35/47	163/32	4.0	304	35.7	237/20	333/16	12.6
57	29.9	310/72	141/18	2.4	119	7.2	95/52	298/34	2.0	181	8.7	250/38	61/45	1.8	243	12.0	305/9	36/18	2.4	305	36.9	264/79	27/8	2.2
58	26.9	148/53	307/35	2.1	120	7.6	206/30	†	1.4	182	9.8	353/61	162/28	6.0	244	59.2	133/50	236/11	2.8	306	39.4	63/63	195/18	12.2
59	29.7	134/60	302/30	3.1	121	11.0	88/5	323/79	4.1	183	9.5	201/48	332/32	2.9	245	26.2	119 /25	22/17	3.4	307	45.3	205/25	350/60	4.4
60	25.9	155/48	324/41	4.9	122	7.4	256/18	3/43	3.6	184	14.3	†	312/18	2.0	246	37.7	32/14	199/65	9.8	308	29.6	61/12	330/4	3.3
61	27.8	125/49	303/41	3.3	123	8.0	229/14	79/72	4.5	185	7.6	211/6	305/39	1.8	247	45.7	115/30	347/44	3.7	309	41.2	68/19	162/10	3.0
62	22.2	87/67	271/23	3.0	124	10.6	215/8	109/62	4.4	186	7.3	272/0	†	2.4	248	43.4	97/29	346/32	4.9	310	6.5	235/22	4/58	3.1

*K = magnitude of the magnetic susceptibility; K_1 = azimuth and plunge (in degrees) of the magnetic lineation; K_3 = azimuth and plunge of the pole of the magnetic foliation; P_{para}% = anisotropy magnitude; †indicates a non-significance, discarded measurement.

MAGNETIC SUSCEPTIBILITY AND COMPOSITIONAL ZONATION

The magnetic susceptibility of the Cauterets–Panticosa granitoids was determined from 310 stations distributed as regularly as possible over the plutons: 79 in E-Cauterets, 122 in W-Cauterets and 109 in Panticosa (Fig. 2). Two cores were drilled at each station and two specimens taken from each core. The bulk susceptibility value, K, for a given station was obtained by averaging the four individual measurements achieved with a Kappabridge susceptometer. The K values of the Cauterets–Panticosa rocks are rather low, almost always less than 50×10^{-5} SI (Table 1). This points to the absence of ferromagnetic minerals, especially magnetite. Therefore these rocks, like most granitoids of the Pyrenees, are dominantly paramagnetic and their susceptibility is mainly due to the iron-bearing silicates, biotite and amphibole. In such granites, K is directly correlated with the iron content and, therefore, with the petrographic type (Gleizes *et al.*, 1993). This is well illustrated in the present case by the outstanding correlation observed between the independently mapped out lithological zonation (Debon, 1972) and susceptibility zonation of the Cauterets–Panticosa complex (Fig. 3a & b).

The following correlations can be established between the magnetic susceptibilities and the petrographic types defined by Debon (1972):

$K < 5 \times 10^{-5}$ SI = fine-grained leucogranite and tourmaline-bearing aplite;

5×10^{-5} SI $< K < 10 \times 10^{-5}$ SI = monzogranite with biotite $\pm$ muscovite $\pm$ cordierite;

10×10^{-5} SI $< K < 20 \times 10^{-5}$ SI = light-coloured granodiorite with biotite $\pm$ amphibole;

20×10^{-5} SI $< K < 30 \times 10^{-5}$ SI = dark granodiorite with biotite and amphibole;

$K > 30 \times 10^{-5}$ SI = quartz-diorite and quartz-gabbro with biotite and amphibole $\pm$ pyroxene.

The transitions between the lithological types are generally gradual. However, sharp contacts have been found in the core zones of the plutons, especially the contacts with the leucogranites and aplites, which appear as cross-cutting bodies. Sharp contacts also bound heterogeneous masses of quartz-diorites and quartz-gabbros included in more felsic facies, particularly in the 'heterogeneous domains' defined by Debon (1972) in the two Cauterets plutons. These masses are characterized by high susceptibility magnitudes (40×10^{-5} SI $< K < 50 \times 10^{-5}$ SI).

In Panticosa, the variation of the concentric zonation is progressive from a monzogranite type in the core zone to quartz-diorites at the periphery. The dense sampling of this pluton (Santana *et al.*, 1992) has allowed us to trace intermediate iso-susceptibility contours at 15×10^{-5} and 25×10^{-5} SI (Fig. 3b) that mirror the lithological zoning. The E-Cauterets pluton also displays a normal concentric zonation, that is

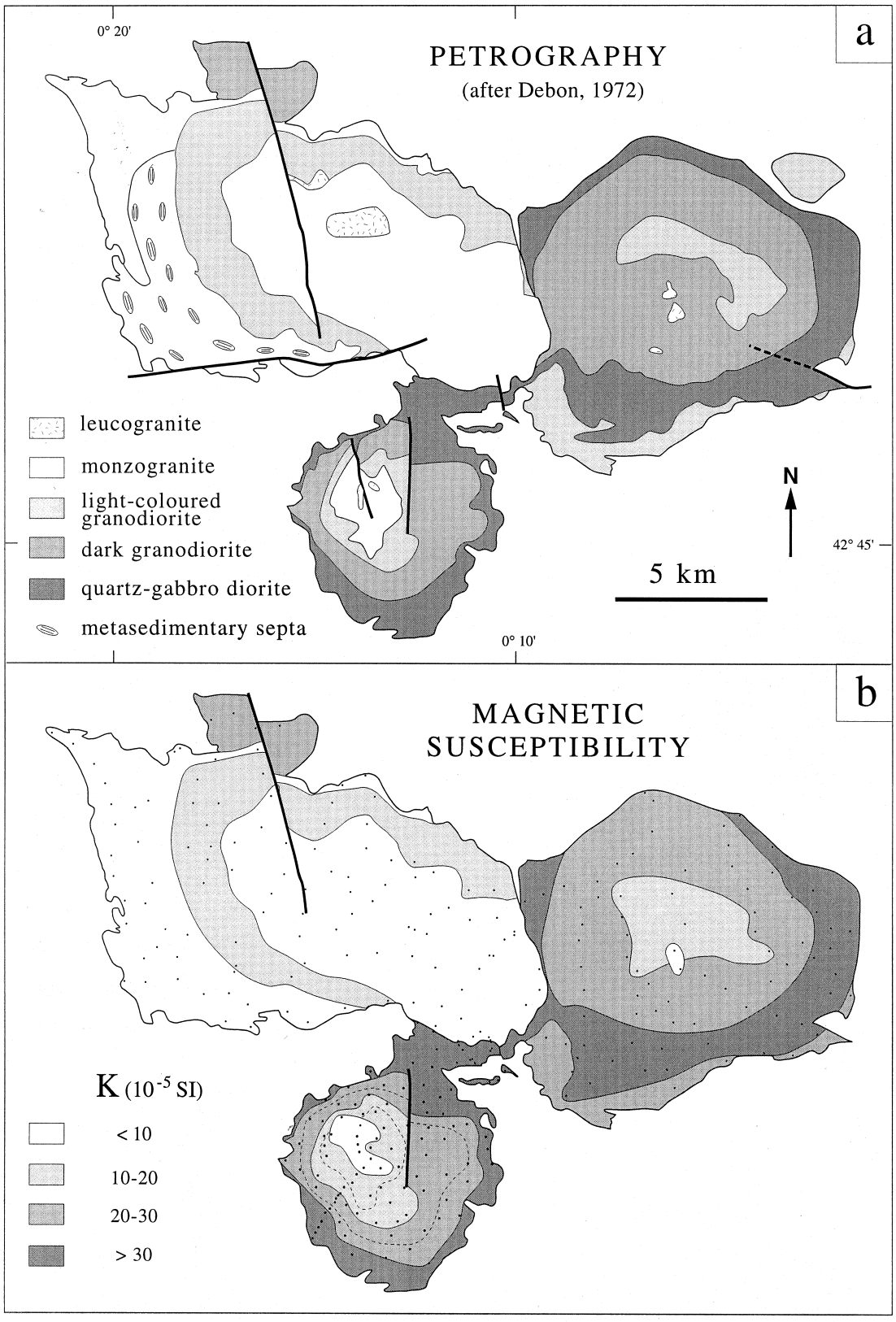

Fig. 3. Maps of the Cauterets–Panticosa complex pointing out the correlation between the petrographic types (a), and the susceptibility values (b). In (b) the dots are the AMS sampling stations and the broken lines in the Panticosa pluton are intermediate iso-susceptibility contours at 15×10^{-5} and 25×10^{-5} SI.

with more felsic types in the core, but the zonation is not as perfect as in Panticosa, particularly in the southern border zone as underlined by the quartz-diorites sandwiched between granodiorites (Fig. 3).

The lithological distribution of W-Cauterets is more complex and differs from the two other plutons by showing no progressive zonation, but rather the juxtaposition of three main petrographic types. The porphyritic monzogranite of the core zone is in sharp magmatic contact to the east and south with the E-Cauterets and Panticosa plutons. Everywhere else this monzogranite is surrounded by a granodiorite with a magmatic but clear-cut contact between them. The pluton ends to the west in a half-ring of monzogranite, whose northern part is homogeneous and comparable to the central monzogranite. Its southern part, however, is very heterogeneous, characterized by mingling of various igneous petrographic types and by numerous septa of metasedimentary country rocks (Fig. 3a). Note also that, to the north of W-Cauterets, a dark granodiorite constitutes an isolated appendix.

STRUCTURES OF THE PLUTONS

The magmatic fabrics, and especially the linear structures, of the Pyrenean granitoid rocks which generally have homogeneous textures and are poorly anisotropic, are particularly difficult to define in the field. To overcome this difficulty, the samples from the 310 stations in the complex have been subjected to anisotropy of magnetic susceptibility measurements (Table 1). The AMS technique is powerful because the rock-AMS ellipsoid, defined by its three main axes $K_1 \geq K_2 \geq K_3$, directly reflects the mineral fabric of the granites (Jover and Bouchez, 1986; Borradaile, 1988; Bouchez, 1997). In the case of biotite $\pm$ amphibole-bearing granites, like the Cauterets complex, the magnetic lineation K_1 is parallel to the zone axis of the biotites and to the mean elongation of the amphiboles; K_3 is perpendicular to the magnetic foliation, which is the mean preferred planar orientation of biotites and amphiboles.

Magnetic foliations

The E-Cauterets pluton displays the simplest planar fabric pattern. The foliation trajectories are concentric in map view and more or less parallel to the margins of the pluton (Fig. 4). Only the foliation orientations in the leucogranite bodies of the core are independent of the overall pattern. The orientation diagram of the foliation poles has a maximum at 154°/8° (mean foliation plane at 64° NW 82°) but its tendency for a girdle distribution suggests a zonal arrangement around a low-plunging, ENE–WSW-trending zone axis. With their steep dips and mean NE–SW strikes at the present level of erosion, the foliations may form an elliptical, funnel-shaped pattern, with an axial plane steeply dipping to the north.

The Panticosa pluton also displays foliations mostly striking NE–SW, but their trajectories are not concentric. Instead, their pattern is sigmoidal and completely oblique on both the lithological limits and the northeast and southwest borders of the pluton (Fig. 4). However, on approaching the contact with the W-Cauterets pluton, the foliations become parallel to the contact. The foliations of the late leucocratic granites ($K < 10 \times 10^{-5}$ SI; within the light-dashed limits of Fig. 4) strike E–W, oblique to the general trend. The diagram of the foliation poles shows two distinct maxima at 326°/40° and 154°/41°, corresponding respectively to the northeastern and southwestern parts of the pluton. However, the mean pole at 151°/12° (mean foliation plane at 61° SE 78°) is very close to the mean pole measured in E-Cauterets.

The W-Cauterets pluton is more complex because it includes two distinct structural bodies, separated by a clear discontinuity of their foliation trajectories. This discontinuity coincides with the southern and western boundary between the granodiorite and the central monzogranite. The latter displays a domed structure, WNW–ESE in elongation, with outward dips, gentle at the core and moderate at the limbs. To the west of the discontinuity, the granodiorite and external monzogranite exhibit a concentric pattern of foliations which are subparallel to the pluton border and steeply dipping. These foliations are truncated by the central dome of monzogranite. However, in the northern part of the W-Cauterets pluton, all the structures become concordant. The diagram of the foliation poles for the whole pluton is not particularly well organized. Nevertheless, a maximum appears at 157°/36°, that is at nearly the same azimuth as in both the other plutons, indicating that the corresponding mean foliation, NE–SW in strike, is the most common orientation of the whole complex.

Magnetic lineations

The linear patterns of the three plutons are characterized by the predominance of the NE–SW trends. The general tendency in the whole complex is the curvature of the lineation trajectories which form sigmoids irrespective of both the contacts between plutons and the lithological limits inside them, even in the late and cross-cutting leucogranite bodies.

In E-Cauterets, the lineation plunges are gentle either towards the northeast or southwest (mean lineation at 235°/2°). Along the northeast and southwest borders of the pluton, the lineations bend clockwise towards N120°E to become parallel to the adjacent borders, hence displaying rather continuous sigmoidal trajectories. However, in the southwest corner of the pluton, where there is an abrupt change of the foli-

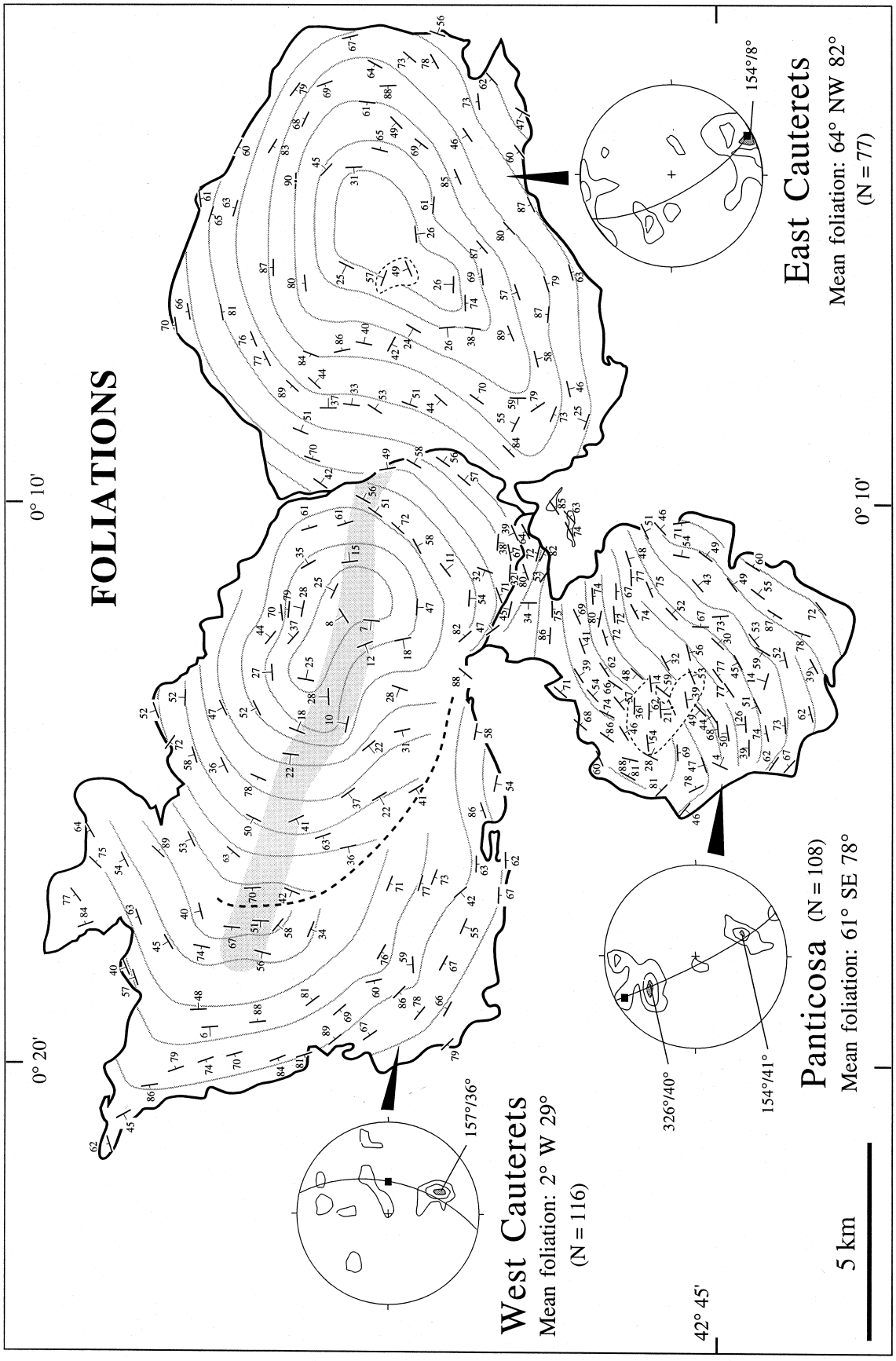

Fig. 4. Map of foliations and foliation trajectories, and diagram of the foliation poles for each pluton (Schmidt, lower hemisphere, 1% area contours). Light shading: location of the northern WNW–ESE-lineation corridor of W-Cauterets which does not disturb the foliation; heavy dashes (W-Cauterets): discontinuity line between foliations; light dashes (Panticosa): limit of late leucogranite (see Fig. 3b).

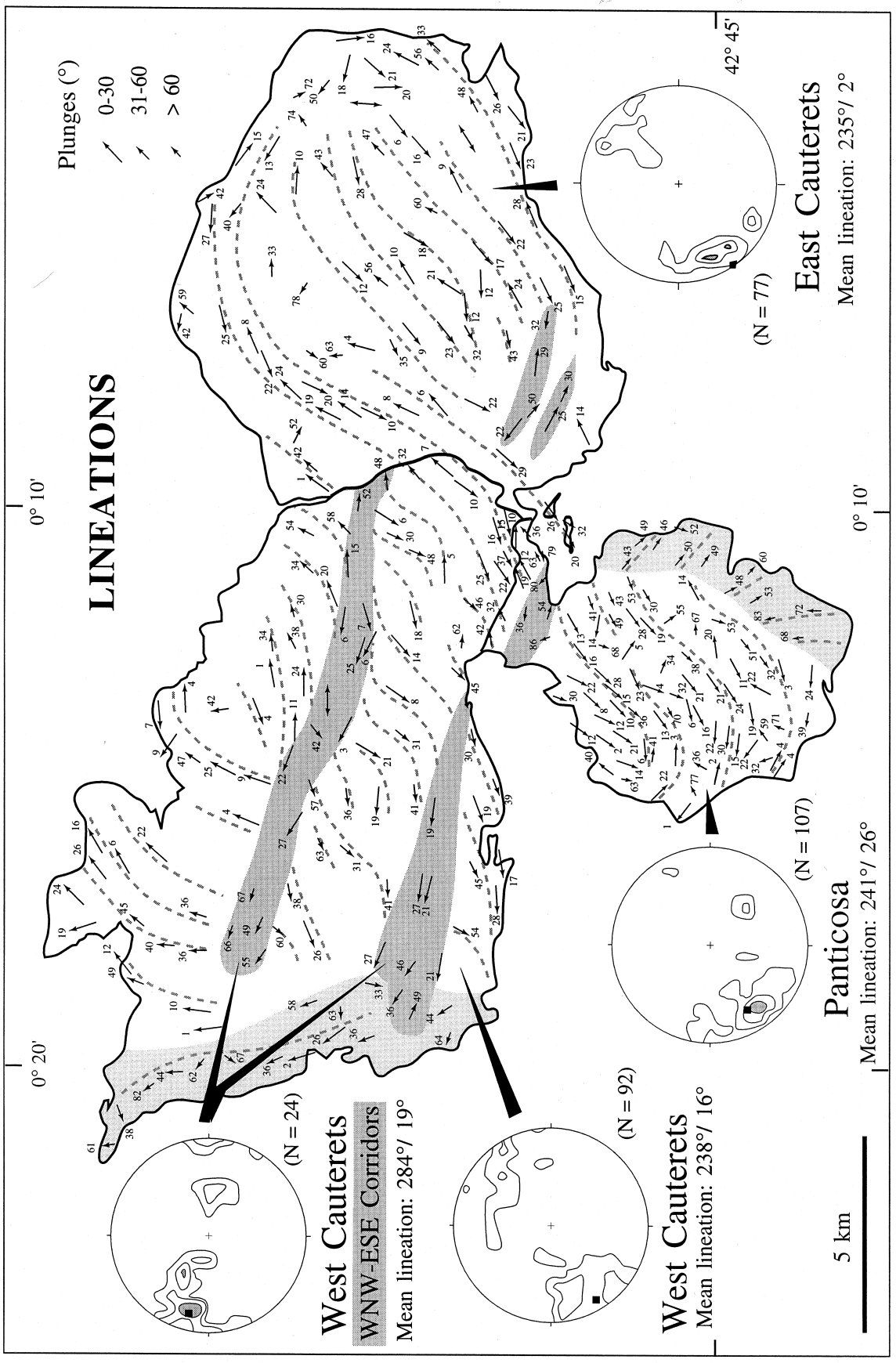

Fig. 5. Map of lineations and lineation trajectories, and diagrams of the lineations (Schmidt, lower hemisphere, 1% area contours). For W-Cauterets, the lineations inside the two WNW–ESE corridors (dark shading) have been distinguished from the others in a separate diagram. Light shading: areas with particular lineations along the eastern border of Panticosa and the western border of W-Cauterets.

ation strikes, this discontinuity is also observed for the lineation trends.

In Panticosa, the lineations also plunge gently, almost always to the southwest (mean lineation at 241°/26°) and depict sigmoidal trajectories that are subparallel to the foliation trajectories. A contrasting lineation trend is observed along the eastern border of the pluton (Fig. 5: light grey shading). These lineations plunge steeply down the foliation dips, mainly to the southeast. Finally some lineations, concentrated in a corridor in the northern part of the pluton (Fig. 5: heavy grey shading), trend approximately WNW–ESE with various plunges.

In W-Cauterets, the preferred linear trends remain NE–SW although, in contrast to the other plutons, they are oblique with respect to the overall foliation trajectories. Surprisingly, the discontinuity that was observed between the central monzogranite and the western lithological units for the foliation trajectories (Fig. 4) is not observed in the lineations. Along the western border of the pluton (Fig. 5: light grey shading), the lineations are parallel to the border and plunge rather steeply to the north. The lineations of the whole pluton can be split into two groups. The most widespread group, corresponding to lineations plunging to the northeast or southwest, displays a 238°/16° mean orientation, that is very close to the mean lineation of E-Cauterets. The second group, with a 284°/19° mean orientation, belongs to two distinct WNW–ESE-trending corridors (Fig. 5: heavy grey shading). One of these corridors is located near the southern border of the pluton. The second corridor roughly coincides with the symmetry axis of the central monzogranitic dome, but extends westward beyond the limit of the monzogranite. Note that at this western extremity of the corridor the lineations are steeply plunging to the west. Finally, one interesting aspect of the lineation pattern of the W-Cauterets pluton is the presence of S-shaped sigmoids of the lineation trends, mainly in-between but also on the sides of the corridors.

MICROSTRUCTURES OF THE PLUTONS

An accurate interpretation of the internal structures of a pluton requires a detailed study of its microstructures in order to determine if the deformation took place in the magmatic state or in the solid state (high or low temperature). In accordance with several other studies dealing with the microstructures present in granitic rocks (Bouchez *et al.*, 1981; Paterson *et al.*,

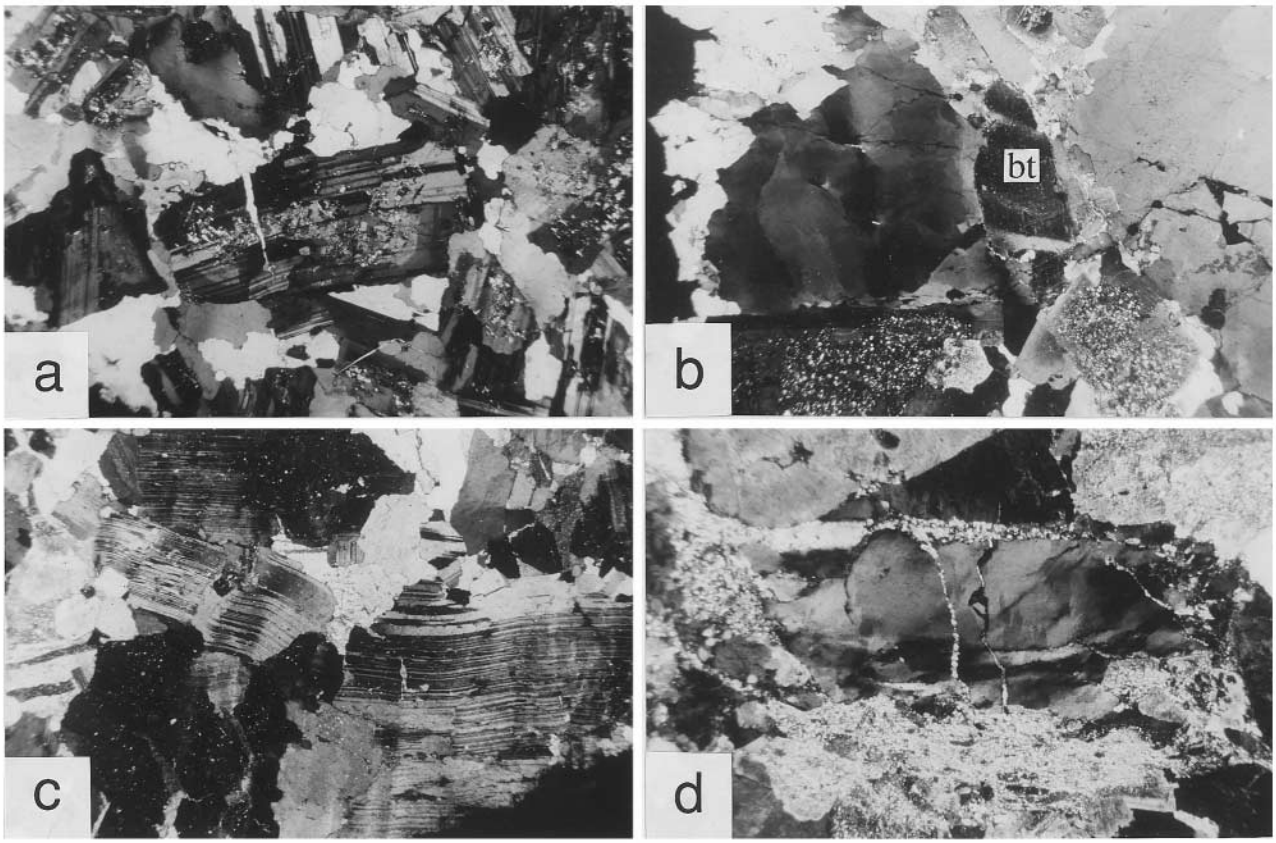

Fig. 6. Photographs of microstructures: (a) submagmatic state with quartz infilling a fracture of the central plagioclase crystal; (b) high-temperature solid state with chessboard-like pattern in quartz and a kinked biotite (bt); (c) high-temperature solid state with bent plagioclases; (d) low-temperature superimposed straining: quartz grain with high-angle undulose extinctions and small quartz grains recrystallized within fractures; note also the phyllosilicates of the matrix. Length of the photographs is 4 mm.

1989; Leblanc *et al.*, 1994, among others), the following types of microstructures are defined.

Magmatic

In the magmatic microstructural type, feldspar crystals are absolutely undeformed and the quartz grains display no more than minor local undulose extinction. In some rocks signs of deformation, which occurred around the solidus, have been observed mainly in the form of plagioclases being fractured with infills of residual melt material characterized by quartz ± feldspar (Fig. 6a), thus defining the submagmatic state of Bouchez *et al.* (1992). The other crystals remain undeformed with the exception of some bends in biotites and subgrain boundaries in quartz. Such a microstructure calls for mechanical interactions between crystals in a magma where the residual melt content was possibly much less than 30% (Arzi, 1978; Fernandez and Barbarin, 1991).

High- to moderate-temperature solid state

Microstructures of this type correspond to a strain imprint, always of a moderate magnitude, that occurred by the end of and/or shortly after the complete crystallization of the magma. The straining of the quartz grains is typical of high-temperature plastic deformation, exhibiting mosaics of square subgrains and forming chessboard-like patterns (Fig. 6b). These subgrains evolve into new grains often with irregular boundaries due to grain-boundary migration. The high-temperature deformation is also attested to by some bends in plagioclases (Fig. 6c), and by the development of kinks in biotite crystals which are not transformed into chlorite.

Low temperature

In this microstructural type, high-angle undulose extinctions and subboundaries are ubiquitous in quartz, along with biotite being transformed into chlorite, and plagioclase partly replaced by sericite. This type of deformation sometimes increases within shear bands, a few tens of metres wide, in which rock straining is readily observed in the field. In these rocks optical microscopy reveals that the size of the recrystallized grains is particularly small, and that these small grains are mostly distributed along the boundaries and within wrench fractures of the original large

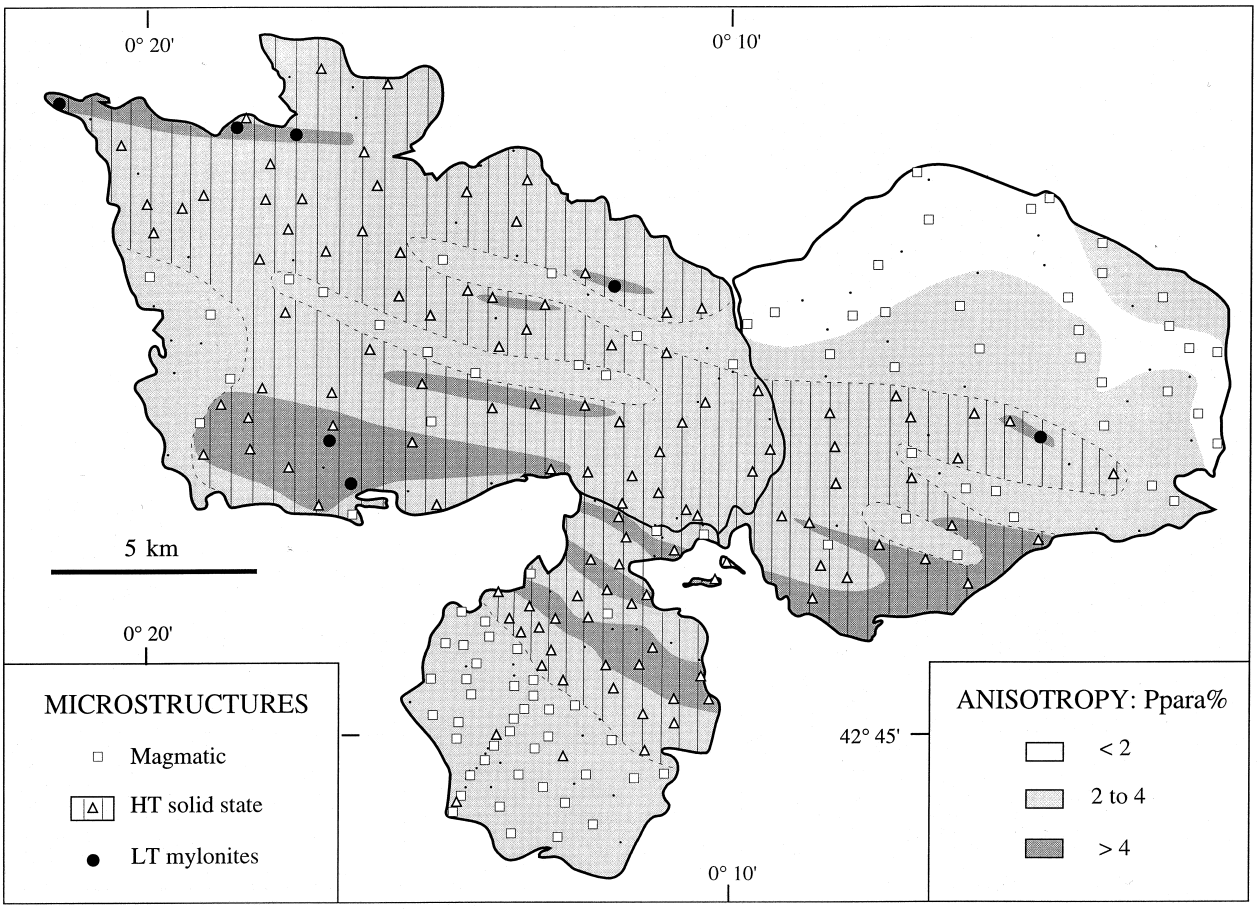

Fig. 7. Distribution map of the microstructural types and of the anisotropy values inside the plutons. Note that the high anisotropy bands are concentrated within a wide WNW–ESE shear zone located in-between the plutons of Cauterets and the pluton of Panticosa.

grains of quartz (Fig. 6d). In places within these shear bands true mylonitic microstructures are observed in which fractured quartz porphyroclasts, included in a matrix dominated by phyllosilicates, are the only remnants of the original granite texture.

Figure 7 reports the map distribution of these microstructural types, as observed with the microscope in thin sections coming from about 75% of the sampling stations. The distribution of these microstructural types in E-Cauterets and Panticosa constitute a striking feature: the northern half of E-Cauterets and the southern half of Panticosa display only magmatic microstructures. These areas are symmetrically disposed with respect to the high-temperature solid-state microstructures which predominate in the south of E-Cauterets and in the north of Panticosa. In W-Cauterets, high-temperature solid-state microstructures are ubiquitous, and this is the case even within the two main corridors where WNW–ESE-trending lineations dominate. However, magmatic microstructures are preserved along two narrow bands outcropping on each side of the northern corridor. Finally, low-temperature and/or mylonitic microstructures are scarce in the whole complex. They are only observed in narrow bands, such as along the northwest border of W-Cauterets.

MAGNETIC ANISOTROPY

In granites devoid of magnetite, that is where the low-field magnetic signature relates almost entirely to the paramagnetic iron-bearing silicates, the anisotropy parameter is defined as $P_{para}\% = 100\ [(K_1{-}D)/(K_3{-}D) - 1]$ in which K_1 and K_3 are the maximum and minimum susceptibilities, and D is the diamagnetic contribution considered to be constant and isotropic, and estimated as -1.4×10^{-5} SI (see Bouchez, 1997). In such granites, a correlation is expected between the bulk magnetic anisotropy and the fabric intensity, itself linked to the accumulated strain magnitude undergone by the rock in the magmatic and solid states (Hrouda, 1982; Benn, 1994; Borradaile and Henry, 1997). Therefore, the map distribution pattern of the anisotropy percentages complements the information coming from the deformation microstructures (Fig. 7).

The mean anisotropy percentages in Panticosa (mean $P_{para}\% = 3.6$) and W-Cauterets (3.5%) are alike. Mean $P_{para}\%$ is substantially lower in E-Cauterets (2.8%) whose northern part has the lowest anisotropies ($< 2\%$) of the whole complex, correlating with absolutely undeformed magmatic microstructures. Intermediate anisotropy magnitudes, between 2 and 4%, are ubiquitous and correspond to microstructures of both magmatic and high-temperature solid-state types. A somewhat irregular distribution in map view of the highest anisotropies ($> 4\%$) underlines the heterogeneity of the solid-state deformation in some areas scattered inside the complex. However, high anisotropy percentages predominate in several WNW–ESE-trending bands which are essentially located in the south of the W- and E-Cauterets plutons and in the north of Panticosa. These bands more or less coincide with corridors where the lineations have the same WNW–ESE trends, unambiguously calling for a strain localization significance of these bands within a main shear zone. By contrast, the northern corridor of W-Cauterets does not coincide with high anisotropy magnitudes. Note finally that while the mylonitic microstructures are confined within high magnetic anisotropy bands, these bands typically contain more commonly high-temperature solid-state microstructures and may even contain magmatic microstructures. This variety of microstructures therefore strongly suggests that the high anisotropy bands have been initiated early during magma crystallization and have further evolved into shear zones that became narrower, hence localized strain, during magma cooling.

COUNTRY ROCK DEFORMATION

The country rocks of the Cauterets–Panticosa complex were metamorphosed to greenschist facies and their bedding planes are often transected by the plutons borders. The regional trajectories of the main foliation of these country rocks strike parallel to the chain, i.e. WNW–ESE, and this orientation is also parallel to the associated fold axes which are subhorizontal on average (Mirouse, 1966; Debon, 1972; Valéro, 1974; Moreau, 1975). All these trajectories are deflected around the plutons, and hence wrap them in map view (Fig. 1). In order to better constrain the emplacement mode of the complex, complementary structural observations have been performed along several N–S transects to the north of the complex, and in the region between the plutons of E-Cauterets and Panticosa.

A single foliation, parallel to bedding, is generally perceived in the field. However, this foliation probably results from the superposition of two events as, in some places, two subvertical foliations are observed at a small angle to each other. The first foliation, S_1, is not easily depicted in the field because it is parallel to the bedding S_0. But S_1 is clearly observed in thin sections where its penetrative character is underlined by the ubiquitous boudinage of S_0 and by pressure shadows around rigid markers. The second planar structure, S_2, is a spaced cleavage which is axial planar to the upright isoclinal folds with horizontal axes, characteristic of the D_2 deformation event. This cleavage, although obvious in the field, is poorly penetrative and difficult to observe in thin sections in such low-grade metamorphic rocks. S_1 and S_2 are generally parallel and thus constitute a composite foliation, $S_{0\text{–}1\text{–}2}$.

The lineations and associated kinematics have been carefully examined. The L_1 lineation, associated with S_1, corresponds to a strong stretching that is usually subvertical. The L_2 lineation, imprinted onto the S_2 cleavage, also indicates stretching, although less conspicuously. It trends E–W and plunges gently to the west, or is subhorizontal, parallel to the axes of the tight folds. Usually, only one type of linear structure is observed at any given place. However, in the few areas exhibiting the two types of lineations, their chronological succession is particularly obvious in the rare hinges of tight folds with subhorizontal axes: the subvertical L_1 is rotated around the D_2 folds, the axes of which are parallel to L_2. In addition, thin sections parallel to L_1 and perpendicular to S_1, i.e. subvertical and N–S in trend, contain evidence of a penetrative non-coaxial deformation, with a systematic top-to-the-south sense of shear. Other sections, parallel to L_2 and perpendicular to S_2, i.e. subhorizontal, also depict a non-coaxial deformation, with a systematic dextral sense of shear.

The D_2 deformation results everywhere in well-imprinted S_2 or S_{0-1-2} foliations. Close to the plutons, the lineations are generally scarce. Their obliteration may be attributed to both strong recrystallization resulting from contact metamorphism, and significant flattening during pluton emplacement. Elsewhere, the imprint of L_2 varies from place to place, whatever the lithology. The regions to the northeast of E-Cauterets and in-between E-Cauterets and Panticosa are characterized by well imprinted horizontal L_2 lineations overprinting L_1 and indicating a strong dextral strike-slip component for D_2. By contrast, in the area north of the pluton of W-Cauterets, only L_1 lineations are observed onto S_{0-1-2} foliations, and the lack of L_2 lineations strongly suggests that D_2 was essentially coaxial there. The contrast between zones where either strike-slip or dominant compression alternate may be the expression of strain partitioning (e.g. Lister and Williams, 1983; Jones and Tanner, 1995) related to a transpressional style of the D_2 deformation.

Finally, the geometric and kinematic features that characterize the two successive tectonic events in the Cauterets–Panticosa area are very similar to those described in other areas of the Pyrenees. Around the Bassiès pluton, it has been shown (Evans *et al.*, 1997) that D_1 was an early southward-thrusting event, characterized by a S_{0-1} foliation originally dipping at low angle, then steepened and folded by E–W folds with horizontal axes during the D_2 shear event. The latter event, also observed in the Trois-Seigneurs area (Leblanc *et al.*, 1996), was concluded to be a dextral and transpressive phase.

DISCUSSION

Interpretation of within-pluton structures

Fabric studies in granites from a variety of geological contexts have established that the magnetic fabric axes are parallel to the mineral fabric axes (e.g. Heller, 1973; Hrouda, 1982; Aranguren *et al.*, 1997; among others), and that these axes record the strain field (flattening plane and stretching direction) to which the magma was subjected, either during its crystallization (magmatic microstructures) or immediately after (high-temperature solid-state microstructures). In the present study, like in many others (see more particularly Saint-Blanquat and Tikoff, 1997), the observation of a continuum between magmatic and high-temperature solid-state microstructures, along with a spectacular continuity in the associated fabrics, points unambiguously to a continuum of magma straining during and just after its crystallization.

The lineations are mainly subhorizontal and organized in sigmoidal patterns (Fig. 5) which, irrespective of the internal lithological boundaries (Fig. 3), are continuous all over the complex, even in the late leucogranite bodies. Therefore, these patterns were acquired after the emplacement of the last magma pulses and represent the recording of a post-emplacement tectonic deformation. The shape of the sigmoids calls for a dextral shearing component for this deformation.

The foliation pattern of Panticosa (Fig. 4) is almost parallel to the lineation pattern and, therefore, is readily interpreted as also due to the regional tectonics. The mean planar orientation being similar in Panticosa and in the two Cauterets plutons, implies that the foliation patterns of the latter plutons must have undergone some 'tectonic' deformation. However, the concentric foliation trajectories of the two Cauterets plutons, like those of most plutons (e.g. Brun and Pons, 1981; Bateman, 1985; Paterson and Fowler, 1993; Ferré *et al.*, 1995) are subparallel to the internal lithological boundaries and also to the external borders. Such planar patterns are considered as resulting from the feeding and expansion of the plutons in their emplacement sites. It is therefore suggested that the planar fabrics retain the memory of kinematic processes slightly older than those retained by the linear fabrics.

In W-Cauterets, the dominantly NE–SW sigmoids of the linear structures extend into two WNW–ESE corridors, where corridor-parallel lineations are observed without any change in the associated microstructures. The development of these corridors is, therefore, unambiguously coeval with the sigmoidal structures. The corridors represent magmatic to high-temperature solid-state shear zones where magma straining was concentrated during the WNW–ESE regional dextral shearing. In the northern corridor, the change of the lineation trends is not associated with

any perturbation of the foliation trajectories. The observation of a planar fabric apparently not disturbed by the deformation responsible for the linear fabric suggests, in this case study, a non-synchronism in the records of the two components of the AMS fabric. This may seem unrealistic as these two components are linked together and should necessarily be both compatible with the last deformational event. However, Borradaile and Alford (1987) and Benn (1994) have shown, by experiments and numerical models respectively, that very small strain overprints, particularly if the compression axis is at a large angle to the original lineation, are sufficient to re-orient this lineation. The latter is the statistically defined zone axis of the biotite grains which corresponds to the finite stretching direction in the foliation plane. A slight modification of the local strain field may easily change this zone axis while, due to the strongly flattened shape of the biotites, their statistical flattening plane which defines the foliation may not be substantially altered. Thus, the northern corridor of W-Cauterets probably represents a km-wide corridor affected by a late magmatic deformation which, while insufficient in magnitude to modify the foliations, was sufficient to re-orient the biotite zone axes from dominantly NE–SW outside the corridor to about N110°E inside. We conclude that, in this particular geometrical situation, the foliation pattern retains the record of magma expansion in its emplacement site while the lineation pattern was more sensitive to late regional deformation.

Syn-emplacement dextral shearing and timing of emplacement

Our structural study allows the establishment of the timing of emplacement of the complex relative to the Hercynian deformation events. Local observations in the country rocks, particularly where deeply imprinted by L_2, strongly argue for an emplacement of the plutons coeval with D_2. In between Panticosa and E-Cauterets, granitic bands and interbedded septa of mica-schists have identical structures which are in continuity with the D_2 structures of the neighbouring country rocks. In XZ-oriented thin sections, the mica-schists exhibit contact metamorphic andalusite crystals with asymmetric pressure shadows which indicate a dextral sense of shear for the deformation that was necessarily coeval with granite emplacement. Regionally, the country rocks display D_2 foliation and fold-axis trajectories that wrap the plutons and form asymmetrical neutral points which point to a dextral regional shear (Fig. 1). This dextral sense of shear is also confirmed by microscopic observations of subhorizontal sections. In the complex itself, the dominant NE–SW structures of the granitic magma, grading towards E–W along the plutons borders and in the corridors and thus forming continuous sigmoids, also call for an emplacement of the plutons during the D_2 dextral shearing event.

This syn-D_2 emplacement age is incompatible with the rather imprecise 290 Ma Rb–Sr age proposed for the complex (Debon, 1975) which is Permian and therefore post-Hercynian. However, it was demonstrated, in other plutons in the Pyrenees, that the Rb–Sr ages cannot be considered as emplacement ages. For example, the previous Permian Rb–Sr ages for the Mont-Louis pluton (275 ± 12 Ma, Vitrac-Michard and Allègre, 1975) and the Bassiès pluton (276 ± 16 Ma, Debon and Zimmermann, 1988) are challenged by recently published U–Pb Carboniferous dates for the same plutons (respectively 305 ± 3 Ma, Romer and Soler, 1995; 312 ± 2 Ma, Paquette *et al.*, 1997). Only these U–Pb ages are compatible with the syn-tectonic emplacement of these plutons, demonstrated by the structural studies (Bouchez and Gleizes, 1995; Evans *et al.*, 1997). Therefore we think that the emplacement of the Cauterets–Panticosa complex, being coeval with D_2, occurred during the Carboniferous.

MODEL OF EMPLACEMENT

In the following model, which attempts to explain the evolution of the three magma bodies forming the complex, a relative chronology of emplacement of the magma types has to be established first. The early emplacement of the more mafic and peripheral types (quartz-diorites, granodiorites) of Panticosa and E-Cauterets is strongly suggested by their less evolved petrographic nature compared to the other types (monzogranites, leucogranites) that grade towards the centres of the plutons. Therefore, and just like most 'normally' zoned plutons showing a progressive petrographic variation, the plutons, while expanding, were fed through their central part by progressively more siliceous magmas. In W-Cauterets, where no progressive zonation is observed, the analysis of the contacts (Debon, 1980) and the truncation of the foliation pattern demonstrate the early emplacement of the granodiorite facies with respect to the monzogranite (Fig. 4). Both cross-cutting contacts in the field and unconformable foliation patterns in map view also apply to the leucogranites which represent the final magma batches found mostly in the centres of the plutons.

The model of Debon (1980), based on a post-D_2 hypothesis for the emplacement of the complex, called for forceful intrusions followed by collapse of the roofs of the E- and W-Cauterets plutons. By contrast, our new structural data call for an emplacement coeval with the D_2 transpressive and dextral shearing event, according to the following sequence (Fig. 8).

1. At the initial stages, and as suggested by the presently subcircular shapes of the plutons, three small magmatic bodies were individually fed by magmas

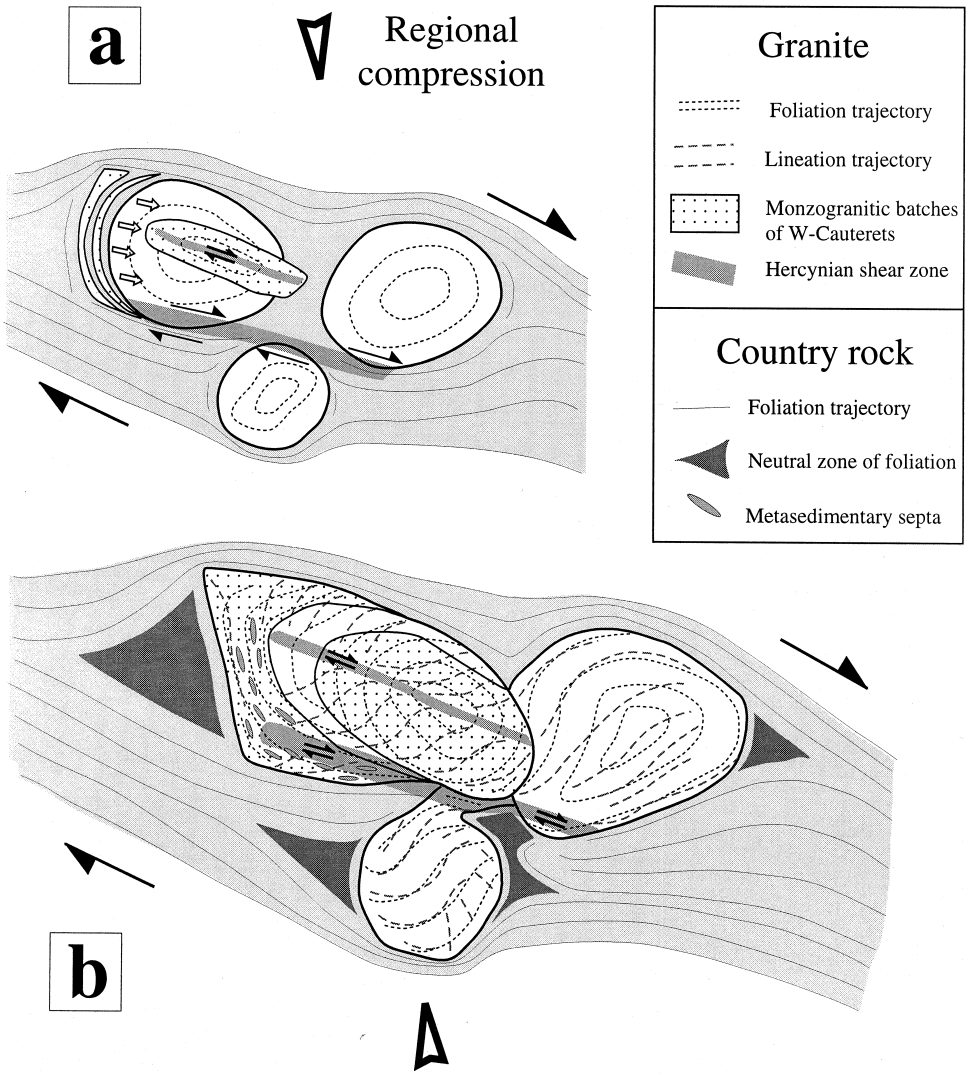

Fig. 8. Model of emplacement and coeval deformation of the Cauterets–Panticosa complex: (a) at the beginning of the intrusion of the last magmatic batches; (b) at the end of magma emplacement.

having the most mafic compositions (quartz-diorites, granodiorites). Their upward motion in this upper crustal, brittle environment probably took place through fractures (Brun *et al.*, 1990; Clemens and Mawer, 1992; Petford *et al.*, 1993). The expansion of the magma reservoirs was mostly a continuous process, as attested by the progressive change of rock compositions, but it was locally discontinuous in places where cross-cutting rock types and foliation trajectories are observed as, for example, in W-Cauterets. This expansion was probably triggered by the WNW–ESE-trending and dextral transcurrent tectonics. However, the precise relationship between pluton inflation and shear zones is not clearly established at these early stages of emplacement.

2. As the plutons increased in size (Fig. 8a), the wide magmatic shear zone that took place in-between the plutons of Cauterets and the pluton of Panticosa (Fig. 8b) triggered the emplacement of the monzogranitic bodies of W-Cauterets, as a consequence of an eastward motion of the granodioritic part of this pluton. The westernmost monzogranite of W-Cauterets had, therefore, the peculiarity of directly intruding the western contact, isolating concentric slivers of country rocks. These slivers parted from one another, without perturbation of their primary stratigraphic succession (Debon, 1972), in a tensional zone comparable with the tensional zones resulting from the opening of a pull-apart or from the horse-tail termination of a strike-slip fault. At that time, the central monzogranite intruded the central part of the granodiorite of W-Cauterets. The WNW–ESE elongation of this monzogranite body and its foliation trajectories, and also the presence of a WNW–ESE-lineated corridor along its symmetry plane, suggest that the feeding of this body occurred along this corridor and during shear movement.

3. The inflating plutons finally became contiguous (Fig. 8b) and the overall dextral shearing was responsible for the sigmoidal lineation trajectories everywhere, and also for the sigmoidal foliation trajectories of Panticosa. In W-Cauterets, the lineation trajectories associated with the WNW–ESE-trending corridors underline *C*–*S*-like patterns attesting to increasing dextral shear strains toward these corridors. The inflation of the central monzogranite of W-Cauterets resulted in a stretching of the enclosing granodiorite and indented the western end of E-Cauterets while both plutons were still partly molten. The main shear zone, to the south of the Cauterets plutons, was responsible for: (i) the further feeding of the westernmost monzogranite whose volume increase lessened the proportion of the included country rock slivers which became boudinaged at the regional scale; (ii) the high-temperature solid-state straining of the southern parts of the two Cauterets plutons and the northern part of Panticosa; (iii) the large anisotropy magnitudes along more localized shear corridors; and (iv) the intense non-coaxial deformation observed in the country rocks in-between E-Cauterets and Panticosa. In short, shear strain along this main shear zone, which probably began early in the emplacement process of the plutons, became localized into progressively narrower bands during the cooling of the magma. Low-temperature mylonites, however, which are located in narrow bands occasionally independent of the high-temperature shear bands, could result from the Alpine deformation event which may have re-used the Hercynian shear planes.

CONCLUSION

The structural patterns observed in both the Cauterets–Panticosa complex and its country rocks give a fine illustration, at the map scale, of simultaneous intrusions and deformation of magmas in a dextral transcurrent setting.

This study emphasizes the ubiquitous sigmoidal pattern of the lineation trajectories as a distinctive and unique feature of the complex. In the Panticosa pluton, the sigmoids of lineations run throughout the pluton and trend parallel to the foliation trajectories. In this case it is inferred that the imprint of the dextral transcurrent regional deformation prevails over the imprint of the magma flow. In the two Cauterets plutons the foliation trajectories remain essentially concentric, and therefore are completely different in shape from the lineation trajectories. In the W-Cauterets pluton the sigmoids of the lineation trajectories do not cut across the whole body, but are confined in-between WNW–ESE-trending shear corridors into which the lineations are deflected towards E–W trends. These corridors do not, however, disturb the foliation trajectories. This implies that the foliations retain the memory of magma emplacement while the lineations express the regional deformation. By the end of magma crystallization, strain became concentrated into the WNW–ESE-trending corridors of the pluton, with no change in the overall dextral transcurrent regime. The presence of only a partial reorientation of the fabric, greater for the lineations than for the foliations, implies a rather low magnitude for this late deformation.

The ubiquitous dextral shear evidenced in the plutons agrees with the kinematics of the D_2 Hercynian event of the Pyrenees. This event was characterized in the country rocks by numerous dextral shear criteria in thin sections and, in map view, by asymmetrical neutral points at pluton tips. This event, which also included a compressive component, was therefore a transpression. These results are fundamental for the understanding of the Hercynian evolution of the whole Pyrenees. Adding the data provided by the study of other plutons, the present results lead to the conclusion that during the D_2 Carboniferous main phase the dextral transpressive strain regime favoured the emplacement of granitoid plutons.

Acknowledgements—We are indebted to the French National Park of Pyrénées authorities who allowed the sampling. We thank François Debon who introduced us to the geology of the Cauterets massif, and Stéphane André, Patrice Bonnafous, Michel de Saint-Blanquat, and Monique and Nicolas Leblanc who participated in the sampling. We also thank Pierre Lespinasse for the AMS measurements, and Christiane Cavaré-Hester and Anne-Marie Roquet for technical assistance in the laboratory. The study has benefitted from discussions with José Maria Tubia and Aitor Aranguren (University of Bilbao) and from the constructive reviews of Edward Sawyer and Antonio Castro. The funding was provided by the CNRS-INSU/DBT programme (France) and by the UPV. 121.310-EB 182/92 project (Spain). This is a contribution of the UMR CNRS/UPS ♯ 5563 'Mécanismes de Transfert en Géologie', équipe Pétrophysique.

REFERENCES

Aranguren, A., Larrea, F. J., Carracedo, M., Cuevas, J. and Tubia, J. M. (1997) The Los Pedroches batholith (southern Spain). Polyphase interplay between shear zones in transtension and setting of granites. In *Granite: From Segregation of Melt to Emplacement Fabrics*, eds J. L. Bouchez, D. H. W. Hutton and W. E. Stephens, pp. 215–229. Kluwer Academic, Dordrecht.

Archanjo, C. J., Bouchez, J. L., Corsini, M. and Vauchez, A. (1994) The Pombal granite pluton: magnetic fabric, emplacement and relationships with the Brasiliano strike-slip setting of NE Brazil (Paraiba State). *Journal of Structural Geology* **16,** 323–335.

Arzi, A. A. (1978) Critical phenomena in the rheology of partially melted rocks. *Tectonophysics* **44,** 173–184.

Bateman, R. B. (1985) Aureole deformation by flattening around a diapir during *in situ* ballooning: the Cannibal Creek granite. *Journal of Geology* **93,** 293–310.

Benn, K. (1994) Overprinting of magnetic fabrics in granites by small strains: numerical modelling. *Tectonophysics* **233,** 153–162.

Borradaile, G. J. (1988) Magnetic susceptibility, petrofabric and strain—a review. *Tectonophysics* **156,** 1–20.

Borradaile, G. J. and Alford, C. (1987) Relationship between magnetic susceptibility and strain in laboratory experiments. *Tectonophysics* **133,** 121–135.

Borradaile, G. J. and Henry, B. (1997) Tectonic applications of magnetic susceptibility and its anisotropy. *Earth Science Reviews* **42,** 49–93.

Bouchez, J. L. (1997) Granite is never isotropic: an introduction to AMS studies of granitic rocks. In *Granite: From Segregation of Melt to Emplacement Fabrics*, eds J. L. Bouchez, D. H. W. Hutton and W. E. Stephens, pp. 95–112. Kluwer Academic, Dordrecht.

Bouchez, J. L., Delas, C., Gleizes, G., Nédélec, A. and Cuney, M. (1992) Submagmatic microfractures in granites. *Geology* **20,** 35–38.

Bouchez, J. L. and Gleizes, G. (1995) Two-stage deformation of the Mont Louis–Andorra granite pluton (Variscan Pyrenees) inferred from magnetic susceptibility anisotropy. *Journal of the Geological Society, London* **152,** 669–679.

Bouchez, J. L., Guillet, P. and Chevalier, F. (1981) Structures d'écoulement liées à la mise en place du granite de Guérande (Loire-Atlantique, France). *Bulletin de la Société géologique de France* **23,** 387–399.

Bresson, A. (1903) Etudes sur les formations anciennes des Hautes et des Basses Pyrénées (Haute Chaîne). *Bulletin de la Carte Géologique de France* **93,** 45–322.

Brun, J. P., Gapais, D., Cogné, J. P., Ledru, P. and Vigneresse, J. L. (1990) The Flamanville granite (northwest France): an unequivocal example of a syntectonically expanding pluton. *Geological Journal* **25,** 271–286.

Brun, J. P. and Pons, J. (1981) Strain patterns of pluton emplacement in a crust undergoing non-coaxial deformation, Sierra Morena, Southern Spain. *Journal of Structural Geology* **3,** 219–229.

Clemens, J. D. and Mawer, C. K. (1992) Granitic magma transport by fracture propagation. *Tectonophysics* **204,** 339–360.

Cruden, A. R. and Launeau, P. (1994) Structure, magnetic fabric and emplacement of the Archean Lebel stock, SW Abitibi Greenstone Belt. *Journal of Structural Geology* **16,** 677–691.

Debon, F. (1972) Massifs granitiques de Cauterets et Panticosa (Pyrénées occidentales). *Carte géologique au 1/50,000 et Notice Explicative*. Bureau de Recherches Géologiques et Minières, Orléans, France.

Debon, F. (1975) Les massifs granitoïdes à structure concentrique de Cauterets-Panticosa (Pyrénées occidentales) et leurs enclaves: une étude pétrographique et géochimique. Unpublished Ph.D. thesis, Université de Nancy 1.

Debon, F. (1980) Genesis of the three concentrically-zoned plutons of Cauterets–Panticosa (French and Spanish Western Pyrenees). *Geologische Rundschau* **69,** 107–130.

Debon, F. and Zimmermann, J. L. (1988) Le pluton de Bassiès (Pyrénées, Zone axiale): typologie chimique, âge et remaniements isotopiques. *Comptes rendus de l'Académie des Sciences de Paris* **306,** 897–902.

Evans, N. G., Gleizes, G., Leblanc, D. and Bouchez, J. L. (1997) A new interpretation of the Hercynian tectonics in the Pyrenees based on the detailed examination of structures around the Bassiès granite. *Journal of Structural Geology* **19,** 195–208.

Fernandez, A. and Barbarin, B. (1991) Relative rheology of coeval mafic and felsic magmas: nature of resulting interaction processes and shape and mineral fabrics of mafic microgranular enclaves. In *Enclaves and Granite Petrology*, eds J. Didier and B. Barbarin, pp. 243–275. Elsevier, Amsterdam.

Ferré, E., Gleizes, G., Bouchez, J. L. and Nnabo, P. N. (1995) Internal fabric and strike-slip emplacement of a Panafrican granite of Solli Hills, Northern Nigeria. *Tectonics* **14,** 1205–1219.

Gleizes, G., Leblanc, D. and Bouchez, J. L. (1997) Variscan granites of the Pyrenees revisited: their role as syntectonic markers of the orogen. *Terra Nova* **9,** 38–41.

Gleizes, G., Nédélec, A., Bouchez, J. L., Autran, A. and Rochette, P. (1993) Magnetic susceptibility of the Mont-Louis–Andorra ilmenite-type granite (Pyrenees): a new tool for the petrographic characterization and the regional mapping of zoned granite plutons. *Journal of Geophysical Research* **98,** 4317–4331.

Heller, F. (1973) Magnetic anisotropy of granitic rocks of the Bergell massif (Switzerland). *Earth and Planetary Science Letters* **20,** 180–188.

Hrouda, F. (1982) Magnetic anisotropy of rocks and its application in geology and geophysics. *Geophysical Survey* **5,** 37–82.

Jones, R. R. and Tanner, P. W. G. (1995) Strain partitioning in transpression zones. *Journal of Structural Geology* **17,** 793–802.

Jover, O. and Bouchez, J. L. (1986) Mise en place syntectonique des granitoïdes de l'Ouest du Massif Central français. *Comptes Rendus de l'Académie des Sciences de Paris* **303,** 969–974.

Leblanc, D., Gleizes, G., Lespinasse, P., Olivier, P. and Bouchez, J. L. (1994) The Maladeta granite polydiapir, Spanish Pyrenees: a detailed magneto-structural study. *Journal of Structural Geology* **16,** 223–235.

Leblanc, D., Gleizes, G., Roux, L. and Bouchez, J. L. (1996) Variscan dextral transpression in the French Pyrenees: new data from the Pic des Trois-Seigneurs granodiorite and its country rocks. *Tectonophysics* **261,** 331–345.

Lister, G. S. and Williams, P. F. (1983) The partitionning of deformation in flowing rock masses. *Tectonophysics* **92,** 1–33.

Mirouse, R. (1966) *Recherches géologiques dans la Partie Occidentale de la zone Primaire Axiale des Pyrénées*. Mémoires de la Carte géologique de France, Orléans, France.

Moreau, H. (1975) Essai de géologie structurale dans le Vignemale et les hautes vallées du rio Ara et du gave d'Ossoue. Unpublished Ph.D. thesis, Université de Bordeaux. .

Paquette, J. L., Gleizes, G., Leblanc, D. and Bouchez, J. L. (1997) Le granite de Bassiès (Pyrénées): un pluton syntectonique d'âge westphalien. Géochronologie U–Pb sur zircons. *Comptes Rendus de l'Académie des Sciences de Paris* **324,** 387–392.

Paterson, S. R. and Fowler, T. K. (1993) Re-examining pluton emplacement processes. *Journal of Structural Geology* **15,** 191–206.

Paterson, S. R., Vernon, R. H. and Tobisch, O. T. (1989) A review of criteria for the identification of magmatic and tectonic foliations in granitoids. *Journal of Structural Geology* **11,** 349–363.

Petford, N., Kerr, R. C. and Lister, J. R. (1993) Dike transport of granitoid magmas. *Geology* **21,** 845–848.

Romer, R. L. and Soler, A. (1995) U–Pb age and lead isotopic characterization of Au-bearing skarn related to the Andorra granite (central Pyrenees, Spain). *Mineralium Deposita* **30,** 374–383.

Saint-Blanquat de, M. and Tikoff, B. (1997) Development of magmatic to solid-state fabrics during syntectonic emplacement of the Mono Creek granite, Sierra Nevada batholith. In *Granite: From Segregation of Melt to Emplacement Fabrics*, eds J. L. Bouchez, D. H. W. Hutton and W. E. Stephens, pp. 231–252. Kluwer Academic, Dordrecht.

Santana, V., Bouchez, J. L., Gleizes, G. and Tubia, J. M. (1992) Estructura del pluton granitico de Panticosa (Pirineos). *III Congreso Geologico de España, Salamanca* **2,** 179–185.

Valéro, J. (1974) Géologie structurale du Paléozoïque de la région de Panticosa, Province de Huesca (Espagne). Unpublished Ph.D. thesis, Université de Bordeaux.

Vitrac-Michard, A. and Allègre, C. J. (1975) A study of the formation and history of a piece of continental crust by ^{87}Rb-^{86}Sr method: the case of the French oriental Pyrenees. *Contributions to Mineralogy and Petrology* **50,** 257–285.

Wensink, H. (1962) Paleozoic of the upper Gallego and Ara Valleys, Huesca Province, Spanish Pyrenees. *Estudios Geologicos* **18,** 1–74.

Zwart, H. J. (1979) The geology of the Central Pyrenees. *Leidse Geologische Mededelingen* **50,** 1–74.